JOURNAL OF Materials CHEMISTRY

A ^{119}Sn and ^{151}Eu Mössbauer spectroscopic, magnetic susceptibility, and electrical conductivity investigation of the stannides EuTSn (T = Cu, Pd, Ag, Pt)

Ralf Müllmann,[a] Uta Ernet,[a] Bernd D. Mosel,[a] Hellmut Eckert,*[a] Reinhard K. Kremer,[b] Rolf-Dieter Hoffmann[c] and Rainer Pöttgen*[c]

[a]*Institut für Physikalische Chemie, Universität Münster, Schloßplatz 4/7, D-48149 Münster, Germany. E-mail: eckerth@uni-muenster.de*
[b]*Max-Planck-Institut für Festkörperforschung, Heisenbergstraße 1, D-70569 Stuttgart, Germany. E-mail: rekre@cesux.mpi-stuttgart.de*
[c]*Department Chemie, Ludwig-Maximilians-Universität München, Butenandtstraße 5–13 (Haus D), D-81377 München, Germany. E-mail: rapch@cup.uni-muenchen.de*

Received 2nd January 2001, Accepted 2nd February 2001
First published as an Advance Article on the web 1st March 2001

The title compounds were prepared from the elements by reaction in sealed tantalum tubes in a high frequency furnace. EuCuSn and EuAgSn crystallize with the KHg_2 type structure with a statistical distribution of the copper (silver) and tin atoms on the mercury position. EuPdSn and EuPtSn adopt the TiNiSi type structure, a ternary ordered version of KHg_2. The four stannides show Curie–Weiss behaviour above 60 K with experimental magnetic moments between 7.75(5) and 8.10(5) μ_B/Eu indicating divalent europium. While EuCuSn remains paramagnetic down to 4.2 K, antiferromagnetic ordering is observed for EuAgSn, EuPdSn and EuPtSn with Néel temperatures of 6.0(5), 15.5(5) and 28.5(5) K, respectively. EuPdSn and EuPtSn show metamagnetic transitions at fields of 2.5(2) and 0.8(1) T, respectively. The stannides EuCuSn, EuPdSn, EuAgSn and EuPtSn are metallic conductors. Temperature dependent ^{151}Eu and ^{119}Sn Mössbauer spectroscopic data confirm the magnetic transition temperatures and yield values of the internal (and transferred) magnetic flux densities. A compilation of the ^{151}Eu isomer shifts for the whole series of EuTX (T = transition metal; X = element of the 3rd, 4th or 5th main group) compounds reveals an interesting linear correlation with the electron count.

Introduction

In recent years we have investigated a series of equiatomic intermetallic EuTX compounds (T = post transition metal; X = Ga, Ge, In, Sn). These europium based compounds adopt different crystal structures resulting in a large variety of magnetic properties (see references 1–5, and references therein). Our previous studies on the EuTSn stannides have been focussed mainly on the crystal chemistry of these materials.[6,7] We have now extended these investigations with respect to physical properties. Herein we report on ^{119}Sn and ^{151}Eu Mössbauer spectroscopic data as well as susceptibility and resistivity measurements of EuCuSn, EuPdSn, EuAgSn and EuPtSn. Some physical properties of EuAgSn and EuPdSn have been published earlier by Adroja and Malik[8] and Hossain *et al.*[9]

Experimental

Starting materials for the preparation of EuCuSn, EuPdSn, EuAgSn and EuPtSn were ingots of europium (Johnson Matthey), copper wire (ϕ 1 mm, Johnson Matthey), palladium and platinum powder (200 mesh, Degussa), silver wire (ϕ 2 mm, Degussa) and a tin bar (Heraeus), all with stated purities better than 99.9%. In our original work[6,7] we prepared these stannides in sealed tantalum tubes under inert conditions in a conventional resistance furnace. In the present study we slightly changed the synthesis conditions. The elemental components were sealed under argon in small tantalum tubes in a miniaturized arc-melting apparatus[10] and subsequently annealed in a high-frequency furnace in a water-cooled sample chamber.[11] The tubes were first annealed at the highest power output of the high-frequency generator (Kontron Rotomelt 1.2 kW) for two minutes and subsequently annealed at about 970 K for thirty minutes. This method allows a quick preparation of single-phase products in quantities of about 1 g in contrast to the long annealing procedures in a resistance furnace.

The purity of all samples was routinely checked by Guinier powder patterns using Cu $K\alpha_1$ radiation and α-quartz (a = 491.30 pm, c = 540.46 pm) as an internal standard. A comparison of the experimentally obtained powder diagrams with the calculated ones[12] assuming the lattice parameters and atomic positions of the previous crystallographic investigations[6,7] showed only the Bragg reflections of the respective ternary stannides, and no impurity lines were observed.

The 21.53 keV transition of ^{151}Eu with an activity of 130 MBq (2% of the total activity of a ^{151}Sm:EuF_3 source) was used for the ^{151}Eu Mössbauer spectroscopic experiments. A $Ca^{119m}SnO_3$ source was available for the ^{119}Sn investigations and a palladium foil of 0.05 mm thickness was used to reduce the tin K X-rays concurrently emitted by this source. The measurements were performed in the usual transmission geometry in a commercial helium bath cryostat. The temperature of the absorber could be varied from 4.2 to 300 K and was measured with a metallic resistance thermometer with an accuracy better than $\pm$0.5 K. The sources were kept at room temperature in all experiments. The material for the Mössbauer spectroscopic measurements, the susceptibility and resistivity measurements was taken from the same sample source. The samples were placed within thin-walled PVC containers at a thickness corresponding to about 10 mg Eu cm^{-2}.

DOI: 10.1039/b100055l

Magnetic susceptibility measurements were performed on polycrystalline samples by use of a MPMS SQUID magnetometer (Quantum Design, Inc.) at temperatures between 4.2 and 300 K with magnetic flux densities up to 7 T. Electrical resistivities were measured with a conventional four-point setup according to the van der Pauw technique[13] between 4.2 and 300 K. Small blocks were cut from the larger polycrystalline pieces of EuCuSn ($1.1 \times 1.1 \times 1.5\ mm^3$) and EuAgSn ($1.0 \times 1.0 \times 0.5\ mm^3$) using a diamond wire saw. Since the EuPdSn and EuPtSn samples were extremely brittle, these resistivity data were measured on irregularly shaped pieces of about $1 \times 1 \times 1\ mm^3$ size. Cooling and heating curves were identical within error limits.

Results and interpretation

Crystal chemistry

The crystal structures of the EuTSn stannides are all derived from the well known KHg_2 type structure.[14] EuCuSn and EuAgSn adopt the KHg_2 type structure with a statistical distribution of the copper(silver) and tin atoms on the mercury position. No long-range order was evident from the single crystal X-ray investigations;[7] however, a large degree of short-range order can certainly be expected. EuPdSn and EuPtSn crystallize with the TiNiSi type structure,[15] a ternary ordered version (superstructure) of the KHg_2 type. The palladium(platinum) and tin atoms are fully ordered on the mercury positions. In the structure we observe slightly puckered T_3Sn_3 hexagons. As examples, the structures of EuAgSn[6] and EuPtSn[7] are presented in Fig. 1.

Since the crystal chemistry and chemical bonding of these KHg_2 related compounds has already been discussed in detail,[3,6,7,16] only a brief illustration is given here. The europium atoms as the most electropositive component of these stannides have transferred their two valence electrons to the [TSn] polyanions. To a first approximation, the formulæ of these stannides may be written as $Eu^{2+}[TSn]^{2-}$. The [TSn] polyanions are emphasized in Fig. 1. The shortest interatomic distances occur between the transition metal and the tin atoms. According to extended Hückel band structure calculations,[17,18] the strongest bonding interactions occur between the transition metal and tin atoms, supporting the description of a polyanionic network. In the structures of EuCuSn and EuAgSn the polyanions have a pronounced two-dimensional character (Fig. 1). Due to the strong puckering of the T_3Sn_3 hexagons in EuPdSn and EuPtSn, we observe a distorted tetrahedral environment of the tin and transition metal atoms (Fig. 1). The SnT_4 tetrahedra are condensed *via* common edges and corners leading now to a three-dimensional polyanionic network in which the europium atoms are embedded. More details are given elsewhere.[19]

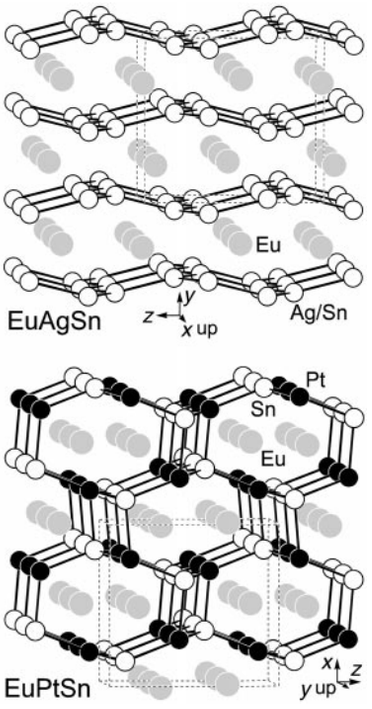

Fig. 1 Orthorhombic crystal structures of EuAgSn (upper) and EuPtSn (lower structure). The europium, platinum and tin atoms are drawn as large grey, small filled and medium open circles, respectively. The mixed occupied Ag/Sn sites in EuAgSn are drawn as medium open circles. The two-dimensionally infinite [AgSn] and the three-dimensionally infinite [PtSn] polyanions are emphasized.

Important parameters for the discussion of the magnetic properties (and the Mössbauer spectroscopic data) are the Eu–Eu distances. The europium atoms form zig-zag chains which thread the tilted T_3Sn_3 hexagons. They extend along the y axis in EuAgSn and along the x axis in EuPtSn. In each compound the Eu–Eu intrachain distances are shorter than the interchain distances (Table 1).

Magnetic and electrical properties

Plots of the inverse magnetic susceptibilities of the four stannides are shown in Fig. 2. Above 60 K the inverse susceptibilities of all compounds follow the Curie–Weiss law. The experimental magnetic moments determined from the data above 60 K vary between 7.75(5) and 8.10(5) μ_B/Eu (Table 1), close to the free ion value of $\mu_{eff} = 7.94\ \mu_B$ for Eu^{2+}. The paramagnetic Curie temperatures (Weiss constants) were obtained by linear extrapolation of the high temperature parts (above 60 K) of the $1/\chi$ *vs.* T plots to $1/\chi = 0$. While positive Weiss constants (indicative of predominant ferromagnetic interactions) of $\Theta = 13(1)$ and 19(1) K were obtained for EuPdSn and EuPtSn, negative values (indicative of predominant antiferromagnetic interactions) of $\Theta = -16(1)$ and $-31(1)$ K were determined for EuCuSn and EuAgSn.

At this point we should comment on the raised magnetic moment of EuPtSn of 8.10(5) μ_B/Eu which is the highest in the series of these equiatomic europium compounds. Similar behaviour is frequently also observed in related gadolinium intermetallics and might be explained in terms of strong coupling (polarization) of the 5d conduction electrons with the gadolinium localized moments.[20,21]

The magnetic susceptibility of EuAgSn has already been determined by Hossain *et al.*[9] In this investigation a large anomaly was detected in the the $1/\chi$ *vs.* T plot at around 70 K. Hossain *et al.* attributed this effect to an oxidation of the material; however, it is clear that such humps in europium based compounds may easily arise from EuO impurities.[22–25] Our studies on the chemical properties of EuAgSn showed a notable resistance of this stannide against humid air over months and the experimental magnetic moment of 7.97 μ_B/Eu determined by Hossain is in good agreement with our data (Table 1). However, the previously reported Weiss constant of about $-5(2)$ K is significantly smaller than the value of $-31(1)$ K determined in the present work. These differences in the magnetic data might be due to a slightly different composition, since the sample of Hossain *et al.* was prepared with an excess of europium (about 5%). A homogeneity range $EuAg_{2-x}Sn_x$ is most likely and has been found in the corresponding gallide systems.[26] The susceptibilities of EuPdSn determined in the present work are in good agreement with the data from Adroja and Malik (8.27 μ_B/Eu, $\Theta = 5$ K and $T_N = 13$ K).[8]

The low temperature behaviour of the inverse susceptibilities is presented in the insets of Fig. 2. No clear indication of magnetic ordering can be deduced for EuCuSn. The sample

Table 1 Crystallographic and magnetic data of EuTSn (T = Cu, Zn, Pd, Ag, Pt, Au). The magnetic data of EuZnSn[4] and EuAuSn[3] were taken from a previous work for comparison. The shortest Eu–Eu and the different Eu–T and Eu–Sn distances in the six structures are listed. μ_{exp}, experimental magnetic moment in the Curie–Weiss region; Θ_P, paramagnetic Curie temperature; T_N, Néel temperature; T_O, ordering temperature determined by ^{151}Eu Mössbauer spectroscopy; B_C, critical magnetic field; $\mu_{sm(exp)}$, experimental saturation magnetic moment at 5.5 T or 7 T

Compound (structure type)	Eu–Eu/pm	Eu–T/pm	Eu–Sn/pm	μ_{exp}/μ_B	Θ_P/K	T_N/K (magn.)	T_O/K (^{151}Eu)	B_C/T (at 2 K)	$\mu_{sm(exp)}/\mu_B$
EuCuSn (KHg_2)	2 × 391.5 2 × 408.3	325.8–344.5	325.8–344.5	7.75(5)	−16(1)	—	11.1	—	3.85(5) at 7 T
EuZnSn (TiNiSi)	2 × 400.0 2 × 414.3	322.5–345.5	332.0–348.3	7.88(5)	24(1)	20.5(2)	26.5(5)	0.7(1)	6.80(5) at 5.5 T
EuPdSn (TiNiSi)	2 × 373.7 2 × 392.5	308.1–338.7	329.4–345.9	7.78(5)	13(1)	T_1 = 15.5(5), T_2 = 6.0(5)	20.8	2.5(2)	6.40(5) at 7 T
EuAgSn (KHg_2)	2 × 388.9 2 × 433.5	335.5–350.2	335.5–350.2	7.96(5)	−31(1)	6.0(5)	6.0	3.5(5)	3.85(5) at 7 T
EuPtSn (TiNiSi)	2 × 374.1 2 × 391.3	309.1–338.8	329.4–345.1	8.10(5)	19(1)	T_1 = 28.5(5), T_2 = 18.0(5)	28.0	0.8(1)	5.80(5) at 7 T
EuAuSn (EuAuSn)	383.7–393.7 416.4–422.4	322.3–351.5	328.4–350.3	7.6(1)	−8(1)	8.5(5)	12(1)	2.0(2)	3.5(1) at 5.5 T

remains paramagnetic down to 4.2 K. The minute anomaly around 33 K is most likely not indicative of magnetic ordering, as illustrated by the magnetization data in Fig. 3 and the Mössbauer data reported below. EuAgSn orders antiferromagnetically at T_N = 6.0(5) K in agreement with the previous investigation of Hossain *et al.*,[9] where magnetic ordering was observed at ~6.5 K. For EuPdSn a Néel temperature of T_N = 15.5(5) K and a second anomaly at 6.0(5) K is evident from Fig. 2. Exactly the same ordering temperature (15.5 K) and also a minute second anomaly at lower temperature is shown in the low temperature plot by Adroja and Malik;[8] however, a lower Néel temperature of 13 K is given in their table. The highest ordering temperature occurs for EuPtSn. The platinum stannide orders antiferromagnetically at 28.5(5) K at an external magnetic flux density of 0.1 T (inset of Fig. 2). A second, small anomaly is observed at 18.0(5) K which may be ascribed to spin reorientations. Similar magnetic behaviour was recently also observed for the isotypic indium compound.[27]

The magnetization *vs.* external magnetic field behaviour of EuCuSn, EuAgSn, EuPdSn and EuPtSn is presented in Fig. 3. At 50 K the magnetization curves are almost linear for all stannides as is expected for paramagnetic compounds. At 2 K the magnetization curves of EuCuSn and EuAgSn remain almost linear, both with a low magnetization of 3.85(5) μ_B/Eu at 7 T, much smaller than the theoretical value of $\mu_{sm(calc)} = 7.0\ \mu_B$/Eu according to $\mu_{sm(calc)} = g \times S\mu_B$.[28] No field induced magnetic transitions are evident for EuCuSn and EuAgSn, similar to EuZnIn[27] and EuAgGe.[2] For EuAgSn, a slight increase of the magnetization is detected above a field strength of 3.5(5) T; however, the effect is too small to be attributed to a field induced magnetic transition.

The low temperature magnetization curves of EuPdSn (4.2 K) and EuPtSn (2 K) are different (Fig. 3). At low flux densities the magnetizations increase monotonically as is expected for an antiferromagnet. The magnetic transitions are observed at field strengths of 2.5(2) T (EuPdSn) and 0.8(1) T (EuPtSn). At the highest accessible field of 7 T the saturation magnetic moments amount to $\mu_{sm(exp)} = 6.40(5)\ \mu_B$/Eu (EuPdSn) and 5.80(5) μ_B/Eu (EuPtSn), somewhat smaller than the maximum value of 7.0 μ_B/Eu. Thus parallel spin alignment of the magnetic moments appears to be dominant at low temperature and 7 T. In contrast, the differently shaped magnetization curves observed for EuPdSn and EuPtSn reveal that the type of spin ordering is different between these materials. Metamagnetism is frequently observed in the series of equiatomic europium transition metal phosphides,

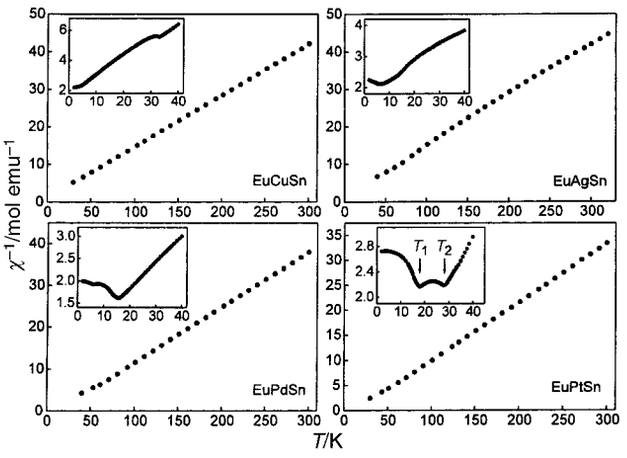

Fig. 2 Temperature dependence of the inverse magnetic susceptibilities of EuCuSn, EuAgSn, EuPdSn and EuPtSn measured at an external field of 2 T. The insets show the low temperature behaviour measured at 0.1 T.

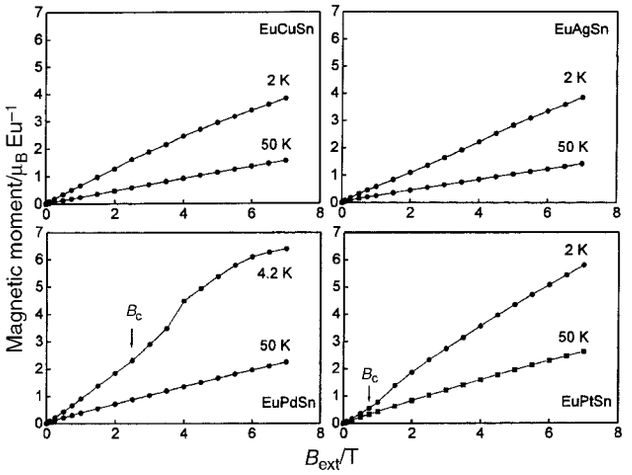

Fig. 3 Magnetization *vs.* external magnetic flux density for EuCuSn, EuAgSn, EuPdSn and EuPtSn at different temperatures. The critical fields B_C for the palladium and platinum compound are indicated.

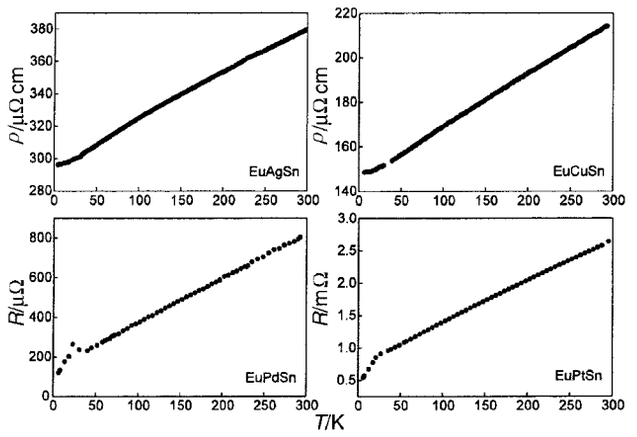

Fig. 4 Temperature dependence of the electrical resistivities of EuCuSn, EuAgSn, EuPdSn and EuPtSn (for details see text).

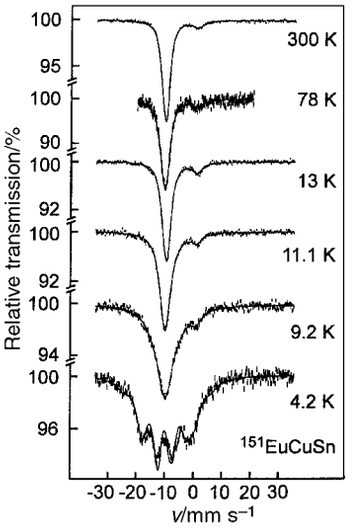

Fig. 5 Temperature dependent ^{151}Eu Mössbauer spectra of EuCuSn. Solid curves denote simulations (see text and Table 2).

arsenides, stannides and indium compounds.[4,27,29,30] The magnetization behaviour of EuAgSn and EuPdSn has not been studied in the previous investigations.[8,9]

The temperature dependence of the electrical resistivity for EuTSn (T = Cu, Ag, Pd, Pt) is shown in Fig. 4. Absolute resistivity values are plotted for EuCuSn and EuAgSn, while the resistance only is given for EuPdSn and EuPtSn. For the latter compounds the polycrystalline lumps were too brittle to be cut into regularly shaped blocks of defined dimensions. The specific resistivities of EuCuSn and EuAgSn decrease linearly from 300 to 4.2 K. No anomalies due to magnetic ordering are visible in the temperature range investigated in agreement with the results of the magnetization investigations. At room temperature the specific resistivities amount to 380 ± 50 μΩ cm (EuAgSn) and 215 ± 50 μΩ cm (EuCuSn).

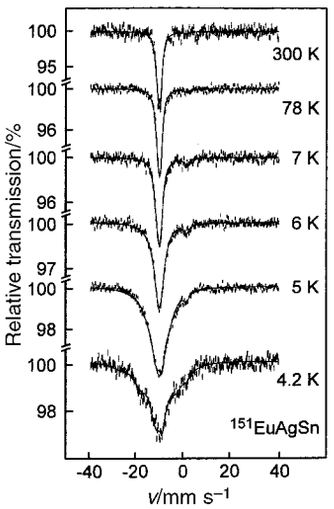

Fig. 7 Temperature dependent ^{151}Eu Mössbauer spectra of EuAgSn. Solid curves denote theoretical simulations (see text and Table 2).

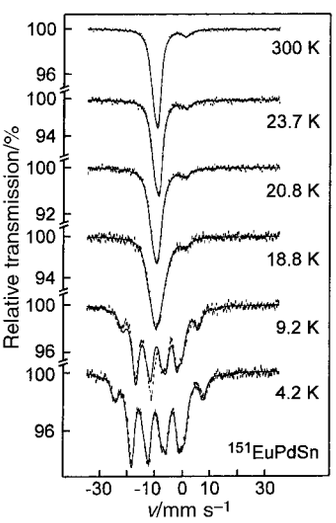

Fig. 8 Temperature dependent ^{151}Eu Mössbauer spectra of EuPdSn. Solid curves denote simulations (see text and Table 2).

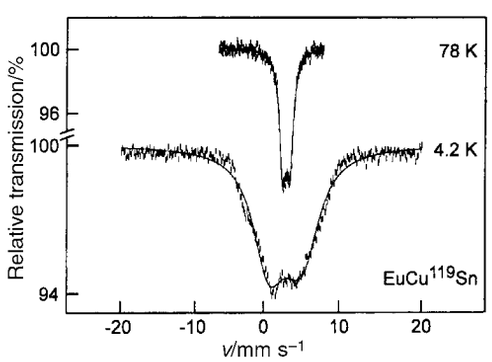

Fig. 6 Temperature dependent ^{119}Sn Mössbauer spectra of EuCuSn. Solid curves denote simulations (see text and Table 3).

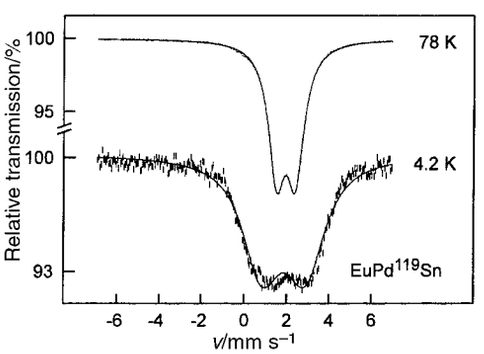

Fig. 9 Temperature dependent ^{119}Sn Mössbauer spectra of EuPdSn. Solid curves denote simulations (see text and Table 3).

Table 2 Fitting parameters of ^{151}Eu Mössbauer measurements in EuTSn compounds (T = Au, Zn, Cu, Ag, Pt, Pd). Numbers in parentheses represent the statistical errors in the last digit. Parameters without parentheses were kept fixed during the fitting procedure. Linewidth parameters (Γ) and isomer shifts (δ) of the different components were coupled. ξ, fraction of magnetic order; $|B_{hf}|$, magnetic hyperfine field; ω, fuctuation frequency; ΔE_Q, electric quadrupole interaction

T/K	δ/mm s^{-1}	Γ/mm s^{-1}	ΔE_Q/mm s^{-1}	$\lvert B_{hf}\rvert$/T	ω/GHz	ξ
EuCuSn						
300	−10.52(2)	2.3	6.5(4)	0	0	0
78	−10.37(8)	2.3	6.3(2)	0	0	0
13	−10.06(3)	2.3	6.3(6)	0	0	0
11.1	−10.23(5)	2.3	−3.2	23.06	15.7(8)	0.10(1)
9.2	−10.08(1)	2.3	−3.2	23.06	4.21(4)	0.32(2)
4.2	−10.17(1)	2.3	−3.2	23.06(6)	2.69(4)	0.79(2)
T/K	δ/mm s^{-1}	Γ/mm s^{-1}	$\lvert B_{hf}\rvert$/T	ξ		
EuZnSn						
300	−10.88(3)	2.3	—	0		
78.0	−10.76(1)	2.3	—	0		
30.0	−10.77(4)	2.3	—	0		
28.0	−10.76(3)	2.3	—	0		
26.0	−10.75(3)	2.3	2.9(2)	0.6(1)		
25.0	−10.75(3)	2.3	4.9(2)	0.8(1)		
20.4	−10.77(5)	2.3	16.9(1)	0.9(1)		
15.7	−10.74(6)	2.3	21.1(2)	1		
11.9	−10.76(5)	2.3	21.5(1)	1		
4.2	−10.76(5)	2.3	23.4(1)	1		
T/K	δ/mm s^{-1}	Γ/mm s^{-1}	ΔE_Q/mm s^{-1}	$\lvert B_{hf}\rvert$/T		
EuPdSn						
300	−9.95	2.21(9)	10.0(4)	0		
23.7	−9.49(5)	2.10(2)	10.0(7)	0		
20.8	−9.88(6)	2.62(2)	−5.0(6)	0.96		
18.8	−9.53(9)	2.64()	−5.1(7)	4.25(3)		
9.2	−9.19(6)	2.54(1)	−5.1	19.22(2)		
4.2	−9.57(5)	2.53(1)	−4.9(6)	22.23(1)		
T/K	δ/mm s^{-1}	Γ/mm s^{-1}	ΔE_Q/mm s^{-1}	$\lvert B_{hf}\rvert$/T	ω/GHz	ξ
EuAgSn						
300	−10.66(2)	1.92(6)	6.0(3)	0	0	0
78	−10.56(8)	2.03(4)	6.2(1)	0	0	0
7	−10.66(1)	2.30(2)	7.4(2)	0	0	0
6	−10.80(1)	2.30	7.4	21.53	8.31(4)	0.17(4)
5	−10.85(1)	2.30	7.4	21.53	4.06(1)	0.41(2)
4.2	−10.86(3)	2.30	7.4	21.53(5)	1.14(5)	0.48(1)
T/K	δ/mm s^{-1}	Γ/mm s^{-1}	ΔE_Q/mm s^{-1}	$\lvert B_{hf}\rvert$/T		
EuPtSn						
78	−9.1(2)	2.62	0	0		
30	9.3(1)	2.62	0	0		
28	−9.3(2)	2.62	0	5.7(5)		
26	−9.1(2)	2.62	0	11.7(5)		
24	−9.3(2)	2.62	0	15.6(4)		
20	−9.2(1)	2.62	0	19.7(4)		
18	−9.1(2)	2.62	0	21.0(4)		
16	−9.2(2)	2.62	0	22.7(4)		
4.2	−9.3(1)	2.62	0	26.2(4)		
T/K	δ/mm s^{-1}	Γ/mm s^{-1}	$\lvert B_1\rvert$/T	$\lvert B_2\rvert$/T	$\lvert B_3\rvert$/T	
EuAuSn						
300	−11.02(3)	2.3	—	—	—	
78.0	−10.86(4)	2.3(1)	—	—	—	
14.7	−10.94(6)	2.2(2)	—	—	—	
13.8	−10.80(5)	2.3(1)	—	—	—	
11.0	−10.73(7)	2.3	7.6(8)	4.3(7)	—	
9.2	−10.68(9)	2.3	14.8(6)	6.1(7)	1.4(5)	
4.2	−10.88(9)	3.5(4)	21.4(6)	10.3(9)	2.2(6)	

The error limits reflect variations among the results obtained for different samples. At 4.2 K the specific resistivities decrease to 78% (EuAgSn) and 70% (EuCuSn) of their room temperature values. The resistance plots of EuPdSn and EuPtSn show anomalies at low temperature, most likely due to freezing of spin-disorder scattering in the magnetically ordered state. These transition temperatures are in agreement with the magnetic data discussed above.

Table 3 Fitting parameters of ^{119}Sn Mössbauer measurements for the stannides EuTSn (T = Au, Zn, Cu, Ag, Pt, Pd). Numbers in parentheses represent the statistical errors in the last digit. Parameters without parentheses were kept fixed. δ, isomer shift; Γ, experimental line width; ξ, fraction of magnetic order; $|B_{hf}|$, magnetic hyperfine field; ω, fuctuation frequency; ΔE_Q, electric quadrupole interaction

T/K	δ/mm s^{-1}	ΔE_Q/mm s^{-1}	Γ/mm s^{-1}	$\lvert B_{hf}\rvert$/T	
EuCuSn					
78	1.99(2)	1.0(3)	1.07(6)	0	
4.2	1.87(7)	−0.5	4.92	3.8(1)	
T/K	δ/mm s^{-1}	Γ/mm s^{-1}	$\lvert B_{hf}\rvert$/T	ξ	
EuZnSn					
300	1.91(1)	1.03	—	0	
78.0	1.94(1)	1.04	—	0	
30.0	1.98(1)	1.02	—	0	
27.0	1.97(2)	1.02	—	0	
26.0	1.98(3)	1.03	2.4(1)	0.4(1)	
25.0	1.96(3)	3.4	3.9(2)	0.8(1)	
18.6	1.97(2)	1.02	9.4(1)	0.9(1)	
13.8	1.97(1)	1.03(4)	11.4(1)	1	
9.2	1.96(1)	1.03(4)	12.4(1)	1	
4.2	1.96(2)	1.04(4)	12.8(1)	1	
T/K	δ/mm s^{-1}	ΔE_Q/mm s^{-1}	Γ/mm s^{-1}	$\lvert B_{hf}\rvert$/T	
EuPdSn					
78	1.98(2)	1.0(4)	0.98(6)	0	
4.2	1.88(4)	0	2.08(2)	1.84(6)	
EuAgSn					
300	1.98(9)	1.10(5)	0.90(4)	0	
78	2.02(3)	1.1(1)	0.96(9)	0	
4.2	1.98(9)	−0.54	5.2(7)	4.0(3)	
EuPtSn					
300	1.85	0.73(2)	0.92(3)	0	
4.2	1.84(3)	0	2.1(1)	1.79(4)	
T/K	δ/mm s^{-1}	Γ/mm s^{-1}	ΔE_Q/mm s^{-1}	$\lvert B_1\rvert$/T	$\lvert B_2\rvert$/T
EuAuSn					
300	1.93(1)	0.98(4)	0.77(3)	—	—
78.0	1.98(2)	1.04(6)	0.76(4)	—	—
15.0	1.99(1)	1.03(5)	0.77(3)	—	—
10.0	1.97(1)	1.52(6)	−0.38	0.7(2)	—
4.2	1.98	1.4(1)	−0.38	8.3(2)	4.2(1)

^{119}Sn and ^{151}Eu Mössbauer spectroscopy

Temperature dependent ^{151}Eu and ^{119}Sn Mössbauer spectroscopic data are given in Figs. 5–10. Transmission integral fits were obtained using the Levenberg–Marquard algorithm, resulting in the parameters isomer shift, electric quadrupolar splitting, line width and internal magnetic flux density. Spectra not affected by magnetic hyperfine splitting (*i.e.* those recorded above the magnetic ordering temperatures) were fitted by single Eu(II) sites subjected to a small axially symmetric electric field gradient. Excessive linebroadening effects observed at some temperatures in EuCuSn and EuAgSn could be successfully reproduced by an uniaxial relaxation model assuming magnetic field fluctuations on the intrinsic timescale of the Mössbauer effect.[31] This model has been previously used successfully to fit the temperature dependent ^{151}Eu Mössbauer spectra of related samples.[2] The fits produce the ordering parameter ξ and the fluctuation frequency ω as additional temperature dependent parameters. Spectra of EuPtSn and EuPdSn were instead fitted assuming a temperature dependent effective magnetic field strength.

Tables 2 and 3 summarize all of the hyperfine parameters resulting from the above fitting procedures. For comparison and completeness, previously published data for the structurally closely related stannides EuZnSn[4] and EuAuSn[3] are also included in the tabulation. For all compounds studied, the isomer shifts indicate europium to be exclusively divalent and no valence fluctuations are observed. In many cases, however, the spectra show a minor component ($<5\%$) in the vicinity of 0.7 mm s^{-1} which is attributed to an Eu^{3+} impurity and is included as a broad Lorentzian in the transmission integral fit at all temperatures. Tin isomer shifts are generally consistent with the values measured for tin in intermetallic compounds. Below the magnetic ordering temperatures, the spectra of all samples show the effects of transferred magnetic hyperfine coupling. However, between different compounds there is a large variation in the magnitude of the transferred magnetic flux density.

Results for EuCuSn are shown in Fig. 5. At temperatures of 13 K and above the ^{151}Eu spectra are well fit by simple Lorentzians. Below 13 K, characteristic linebroadening and splitting in several hyperfine components indicate the onset of magnetic ordering. With the onset of magnetic ordering below T_o the electric field gradient parameter used to optimize the fits changes by the factor −1/2 in EuCuSn, indicating that the principal axis of the electric field gradient tensor is oriented perpendicular to the direction of the magnetic hyperfine field. The Mössbauer spectra below 13 K are well fit by the uniaxial relaxation model assuming fluctuations of B_{hf} perpendicular to the EFG principal axis direction. The corresponding fluctuation frequencies and ordering parameters at the various temperatures measured are included in Table 2. Static magnetic hyperfine splitting is not observed down to a temperature as low as 4.2 K, indicating that the ordering parameter is still substantially below saturation at this temperature. Transferred magnetic hyperfine fields are also clearly apparent as excessive linebroadening effects in the 4.2 K ^{119}Sn Mössbauer spectrum (Fig. 6). The poorly resolved lineshape makes the attainment of a unique fit impossible in this case. This was found to be the

situation in all of the ^{119}Sn Mössbauer spectra recorded at 4.2 K in the present set of samples. This is consistent with the low-temperature ^{119}Sn data of EuAgSn reported by Hossain *et al.*[9] An approximate fit was obtained by assuming perpendicular orientations of the magnetic hyperfine field and the principal axis directions, resulting in an order-of-magnitude estimation of the transferred magnetic hyperfine field strength. For EuCuSn the observation of magnetic hyperfine splitting in the ^{151}Eu and ^{119}Sn Mössbauer spectra stands in contrast to the magnetic susceptibility data, which show no clear evidence of a magnetic ordering transition.

Fig. 7 summarizes the ^{151}Eu Mössbauer spectra of EuAgSn, revealing qualitatively very similar results to those obtained for the copper compound. Indications of magnetic ordering appear at 6.0 K, which is in excellent agreement with the transition temperature deduced from the magnetic susceptibility data. For fitting the temperature dependent ^{151}Eu Mössbauer spectroscopic data set, the uniaxial relaxation model turned out to be most successful. As in EuCuSn, the ordering parameter remains substantially below unity at 4.2 K. Also, the ^{119}Sn Mössbauer spectrum recorded at this temperature reveals very similar features as that of the copper compound with a transferred magnetic flux density in the vicinity of 4 T.

Fig. 8 summarizes the Mössbauer spectroscopic investigations on EuPdSn. The onset of magnetic ordering is detected in the ^{151}Eu data at 20.8 K which is somewhat higher than the temperature seen in the magnetic susceptibility data (15 K). Full magnetic hyperfine splitting is observed at 4.2 K with a magnetic flux density of 22.2 T. Spectra at higher temperatures could be fitted assuming a temperature-dependent effective magnetic flux density rather than relaxation effects. The ^{119}Sn Mössbauer spectra again show the effects of a weak transferred magnetic flux density. The approximate fit shown in Fig. 9 is based on a 54.7° orientation of the internal magnetic field direction with respect to the EFG principal axis.

Fig. 10 shows the ^{151}Eu Mössbauer spectra of EuPtSn. In this compound, linebroadening effects due to the onset of magnetic ordering become apparent at 28.0 K in excellent agreement with the value of T_1 determined from susceptibility measurements. The second magnetic transition at $T_2 = 18$ K is not clearly evident from the Mössbauer data. Rather, a gradual increase of magnetic splitting is observed down to a temperature of 4.2 K, which is fitted by assuming a temperature-dependent effective magnetic flux density. For each spectrum measured above 4.2 K a Lorentzian component at an isomer shift of -10.5 mm s^{-1}, contributing about 10% of the total area, had to be included to produce satisfactory fits. This additional component is attributed to an impurity phase containing Eu(II) in a different electronic and magnetic environment from that of the target compound. The X-ray powder pattern of this sample, however, showed only the reflections from EuPtSn.

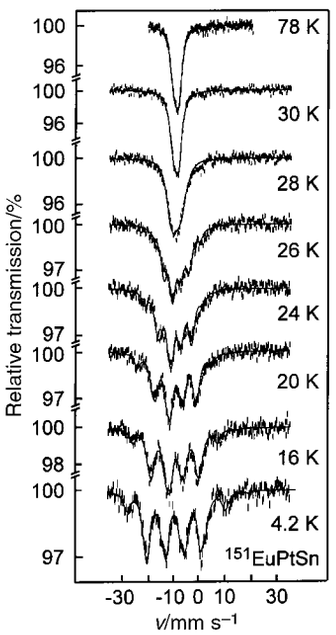

Fig. 10 Temperature dependent ^{151}Eu Mössbauer spectra of EuPtSn. Solid curves denote simulations (see text and Table 2).

Discussion

Manifestations of magnetic disordering

In general, the magnetic transition temperatures determined from the magnetic susceptibility data and from Mössbauer spectroscopy show excellent agreement. A notable exception occurs for the stannide EuCuSn, whose magnetic characterization data show no evidence of any ordering, while the Mössbauer spectra reveal a transition at 11.1 K. A similar situation was previously encountered for the isostructural compound EuAgGe[2] and attributed to cluster glass (micromagnetic) behaviour. Other features, which are common for EuAgGe,[2] EuCuSn, EuAgSn and EuZnIn,[27] are the absence of a field induced magnetic transition along with comparatively low magnetizations at high magnetic field strengths. The Mössbauer spectra of these four compounds reveal a common pattern suggesting structural disordering effects: down to a temperature of 4.2 K the full hyperfine splitting is not attained and magnetic field fluctuation effects must be assumed to provide acceptable fits to the temperature dependent spectra. Furthermore, in the case of EuAuSn[3] and EuAuGe[2] multiple internal magnetic fields had to be invoked to fit the spectra. A detailed inspection of the magnetic and Mössbauer data of all of the EuTX published to date reveals an interesting correlation with their structural characteristics: manifestations of magnetic disorder (such as mentioned above) are observed to varying degrees in all of those compounds that crystallize in the KHg_2 structure, but are never very pronounced in compounds of the TiNiSi type. Both structures differ in the local T and X metal atom distributions surrounding the Eu(II) site: while the TiNiSi type compounds are characterized by strict site ordering, *i.e.* each Eu(II) is surrounded by 6 T and 6 X atoms, in the KHg_2-type compounds the twelve T and X atoms surrounding each Eu site are statistically disordered. As a result of this disorder multiple local environments EuT_nX_{12-n} are probable. On this basis, the magnetic disordering phenomena can be rationalized in terms of local field distributions and/or the formation and dynamic fluctuation of small domains with short range order.

Aside from an order-of-magnitude estimation of the transferred magnetic flux density, the ^{119}Sn Mössbauer spectra do not offer any in-depth information. In particular, it remains uncertain, why in the case of the stannides EuZnSn[4] and EuAuSn,[3] the transferred hyperfine field strengths are so much larger than in the present set of compounds.

^{151}Eu isomer shift trends in EuTX compounds

For the equiatomic indium compounds EuTIn (T = Zn, Rh, Pd, Pt, Au) we recently observed a linear correlation of the ^{151}Eu isomer shift with the shortest Eu–Eu distance in the structure.[32] Comparison of these data with Table 2 reveals that this correlation does not extend to the present set of stannides, although they are structurally closely related. Inspection of the considerable amount of ^{151}Eu Mössbauer data obtained on EuTX compounds during the past five years[33] reveals a much more general correlation with the valence electron count $n(\text{total}) = n(\text{Eu}) + n(\text{T}) + n(\text{X})$, where $n(\text{Eu}) = 2$ according to the ^{151}Eu isomer shift measured. This correlation (which holds

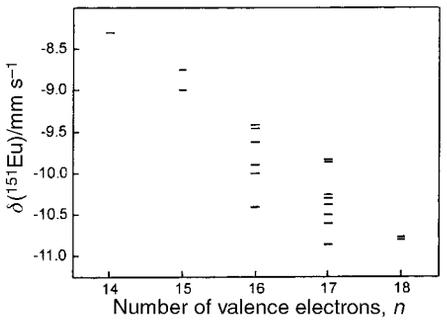

Fig. 11 Plot of the ^{151}Eu Mössbauer isomer shifts measured at 78 K *versus* the total number of valence electrons (VE) for various ternary EuTX intermetallics. Examples are EuRhIn (14 VE), EuPdIn (15 VE), EuPdSn (16 VE), EuAuSn (17VE) and EuZnSn (18 VE).

equally well for the 300 K data and the 78 K data) is shown in Fig. 11 and even includes compounds having different crystal structures and local Eu(II) environments. Given the fact that the size of the ^{151}Eu nucleus increases upon excitation, this trend implies that the effective s-electron density at the nucleus decreases with increasing *n*. The effect can be well understood in terms of previous literature data on ^{151}Eu isomer shifts for Eu(II) in intermetallic compounds. Cashion *et al.*[34] have estimated the isomer shift of a purely ionic Eu(II) species at -11.2 mm s^{-1}. The experimental isomer shift of -7.8 mm s^{-1} measured in europium metal, then, can be attributed to the effect of the density of the conduction electrons at the nuclear sites. In metallic europium, these conduction electrons originate from the 6s orbitals, resulting in a relatively high s-electron density at the nuclei. This interpretation is confirmed by the observation of significant increases in the ^{151}Eu isomer shift as a function of applied pressure.[35] Inspection of available literature data shows that, with very few exceptions, the isomer shifts of binary and ternary Eu(II)-based intermetallic compounds are significantly more negative than that of Eu metal, indicating that the effective s-electron density at ^{151}Eu is significantly reduced.[34] Qualitatively, the effect can be attributed to additional d- or p-valence electron density contributed to the conduction band by the alloying partner,[36] lowering the overall s-character and resulting in more efficient screening. This simple interpretation is supported by several well-documented experimental facts. First of all, in binary compounds EuT_n the isomer shift decreases systematically with increasing *n*, reflecting the effect of decreasing europium density.[37] Secondly, when considering the structurally related compounds EuT_2 and EuX_2 within the same row of T and X elements in the periodic table, the isomer shift decreases systematically as the number of valence electrons increases. For example, within the series $EuCu_2$, $EuZn_2$, $EuGa_2$, $EuGe_2$, the isomer shift values are -7.9, -9.1, -10.2 and -10.5 mm s^{-1}; similar trends are seen for analogous compounds of the 5th and 6th row elements.[35,36] In close analogy to these findings for the binary compounds, the universal relationship between the isomer shift and *n*(total) suggested by Fig. 11 reflects the decrease in average s-character of the conduction band due to the d- and p-valence electron contributions originating from the T and X atoms, respectively.

Acknowledgements

We are indebted to Nicola Rollbühler and Eva Brücher for the help with the susceptibility and resistivity measurements. We also thank Falko M. Schappacher for assistance with the Mössbauer measurements. This work was financially supported by the Deutsche Forschungsgemeinschaft, the Fonds der Chemischen Industrie and the Wissenschaftsministerium Nordrhein-Westfalen.

References

1 R. Pöttgen, *J. Mater. Chem.*, 1995, **5**, 505.
2 R. Müllmann, B. D. Mosel, H. Eckert, R. Pöttgen and R. K. Kremer, *Hyperfine Interact.*, 1997, **108**, 389.
3 R. Pöttgen, R.-D. Hoffmann, R. Müllmann, B. D. Mosel and G. Kotzyba, *Chem. Eur. J.*, 1997, **3**, 1852.
4 U. Ernet, R. Müllmann, B. D. Mosel, H. Eckert, R. Pöttgen and G. Kotzyba, *J. Mater. Chem.*, 1997, **7**, 255.
5 R. Pöttgen, R.-D. Hoffmann and J. Grin, *Z. Kristallogr.*, 1999, **Suppl. 16**, 55.
6 R. Pöttgen, *Z. Naturforsch.*, 1996, **51b**, 806.
7 R. Pöttgen, *J. Alloys Compd.*, 1996, **243**, L1.
8 D. T. Adroja and S. K. Malik, *Phys. Rev. B*, 1992, **45**, 779.
9 Z. Hossain, R. Nagarajan, M. Etilé, C. Godard, J. P. Kappler, L. C. Gupta and R. Vijayaraghavan, *J. Magn. Magn. Mater.*, 1995, **150**, 223.
10 R. Pöttgen, Th. Gulden and A. Simon, *GIT Labor-Fachzeitschrift*, 1999, **43**, 133.
11 R. Pöttgen, A. Lang, R.-D. Hoffmann, B. Künnen, G. Kotzyba, R. Müllmann, B. D. Mosel and C. Rosenhahn, *Z. Kristallogr.*, 1999, **214**, 143.
12 K. Yvon, W. Jeitschko and E. Parthé, *J. Appl. Crystallogr.*, 1977, **10**, 73.
13 L. J. van der Pauw, *Philips Res. Rep.*, 1958, **13**, 1.
14 E. J. Duwell and N. C. Baenziger, *Acta Crystallogr.*, 1955, **8**, 705.
15 C. B. Shoemaker and D. P. Shoemaker, *Acta Crystallogr.*, 1965, **18**, 900.
16 D. Kußmann, R.-D. Hoffmann and R. Pöttgen, *Z. Anorg. Allg. Chem.*, 1998, **624**, 1727.
17 G. Nuspl, K. Polborn, J. Evers, G. A. Landrum and R. Hoffmann, *Inorg. Chem.*, 1996, **35**, 6922.
18 R.-D. Hoffmann and R. Pöttgen, *Z. Anorg. Allg. Chem.*, 2000, **626**, 28.
19 R.-D. Hoffmann and R. Pöttgen, *Z. Anorg. Allg. Chem.*, 1999, **625**, 994.
20 F. Canepa, M. L. Fornasini, F. Merlo, M. Napoletano and M. Pani, *J. Alloys Compd.*, 2000, **312**, 12.
21 C. Felser, K. Ahn, R. K. Kremer, R. Seshardi and A. Simon, *J. Solid State Chem.*, 1999, **147**, 19.
22 B. T. Matthias, R. M. Bozorth and J. H. Van Vleck, *Phys. Rev. Lett.*, 1961, **5**, 160.
23 D. B. McWhan, P. C. Souers and G. Jura, *Phys. Rev.*, 1966, **143**, 385.
24 B. Stroka, J. Wosnitza, E. Scheer, H. v. Löhneysen, W. Park and K. Fischer, *Z. Phys. B: Condens. Matter*, 1992, **89**, 39.
25 R. Pöttgen, R. K. Kremer, W. Schnelle, R. Müllmann and B. D. Mosel, *J. Mater. Chem.*, 1996, **6**, 635.
26 R. Pöttgen and Yu. Grin, *Z. Kristallogr.*, 1996, **Suppl. 11**, 93.
27 R. Müllmann, B. D. Mosel, H. Eckert, G. Kotzyba and R. Pöttgen, *J. Solid State Chem.*, 1998, **137**, 174.
28 A. Szytuła and J. Leciejewicz, *Handbook of Crystal Structures and Magnetic Properties of Rare Earth Intermetallics*, CRC Press, Boca Raton, FL, 1994.
29 C. Tomuschat and H.-U. Schuster, *Z. Anorg. Allg. Chem.*, 1984, **518**, 161.
30 T. Ito, S. Nishigori, I. Hiromitsu and M. Kurisu, *J. Magn. Magn. Mater.*, 1998, **177–181**, 1079.
31 J. A. Tjon and M. Blume, *Phys. Rev.*, 1968, **164**, 456.
32 R. Pöttgen, R.-D. Hoffmann, M. H. Möller, G. Kotzyba, B. Künnen, C. Rosenhahn and B. D. Mosel, *J. Solid State Chem.*, 1999, **145**, 174.
33 R. Pöttgen and D. Johrendt, *Chem. Mater.*, 2000, **12**, 875.
34 J. D. Cashion, M. A. Coulthard and D. B. Prowse, *J. Phys. C*, 1974, **7**, 3620.
35 U. F. Klein, G. Wortmann and G. M. Kalvius, *Solid State Commun.*, 1976, **18**, 291.
36 F. Grandjean and G. J. Long, *Mössbauer Spectroscopy Applied to Inorganic Chemistry*, Vol. 3, Plenum Press, New York, 1989, p. 513.
37 J. W. C. deVries, R. C. Thiel and K. H. J. Buschow, *Physica B+C*, 1983, **121**, 100.